SUBSURFACE DAMAGE FEATURES FOLLOWING PROJECTILE DECAPITATION. A.M. Stickle[1] and P.H. Schultz[1], [1]Brown University Geological Sciences, 324 Brook St., Box 1846, Providence, RI 02912. angela_stickle@brown.edu.

Introduction: A combination of laboratory experiments and numerical simulations reveal subsurface failure patterns in transparent targets [e.g., 1-4]. Two main regions characterize the subsurface failure: a damage region extending below (and uprange from) the impact point and a diving "tongue" downrange [4-5]. Numerical models reveal that plastic shear failure dominates the primary damage region below the impact point. The downrange, diving tongue, however, has not been replicated by these simulations [4]. Here, we experimentally isolate the process responsible for the downrange tongue.

Experimental Approach: The combination of laboratory and numerical experiments allows close examination of subsurface damage in PMMA targets. Numerical simulations provide a way to test conclusions about failure mode and dominant processes seen in small-scale experiments.

Experiments were performed at the NASA Ames Vertical Gun Range (AVGR) in order to isolate the processes responsible for the downrange "tongue" feature. With increasing impact angle (with respect to the horizontal), this downrange feature becomes less pronounced and subtends a smaller angle around the impact point**.** Moreover, the extent of this feature can be matched for identical values of impactor momentum at a given impact angle. Consequently, the momentum vector of the projectile directed downrange plays a role in the formation of the tongue. Further, development of the tongue appears to be related to the failure of the projectile.

Transparent PMMA target blocks were modified to isolate downrange sibling impacts by the decapitated projectile from an oblique impact (15-30°), following [5]. Plasticine clay was pressed into a 5-cm milled shelf in the target and positioned downrange from the impact point. This strategy shielded impacts by projectile fragments (siblings) from impacting the PMMA block downrange and allowed assessing the effects of sibling impacts on the downrange tongue. The shelf depth ranged from 0.158 – 0.3175 cm (corresponding to 0.25-0.5 times the projectile diameter). The Plasticine layer absorbed and/or scattered the energy from the second impact by projectile material [5-6].

Comparisons with three-dimensional CTH models [7] reveal details about the mode of failure. The calculations used a Mie-Grüneisen equation of state (EOS) for the PMMA substrate and the semi-analytical ANEOS [8] for aluminum. The Johnson-Cook fracture model [9] tracks failure within the PMMA target. Plastic failure occurs when the material experiences specified values of plastic strain after it reaches the compressive yield strength. Here, failure is set at 10% strain, benchmarked by comparisons with other impact experiments [4]. Extensional failure (examined separately) occurs when tensional stresses exceed the yield strength of the material.

Results and Discussion: Figure 1 shows the final damage extent and morphology for two impacts with approximately identical impact conditions: 0.635-cm aluminum projectile impacting at ~4.8 km/s at an angle of 15° above the horizontal for an unmodified target (Figure 1, top) and a downrange Plasticine layer over a notched target (Figure 1, bottom). Here, the final damage extent below the impact point is equivalent, and the main damage region grows in the same manner for both target geometries. The downrange, diving tongue is absent for the target with the downrage surface layer, however (Figure 1, bottom). For comparison, three-dimensional, laboratory-scale CTH models of AVGR impacts do not resolve this feature either (Figure 2).

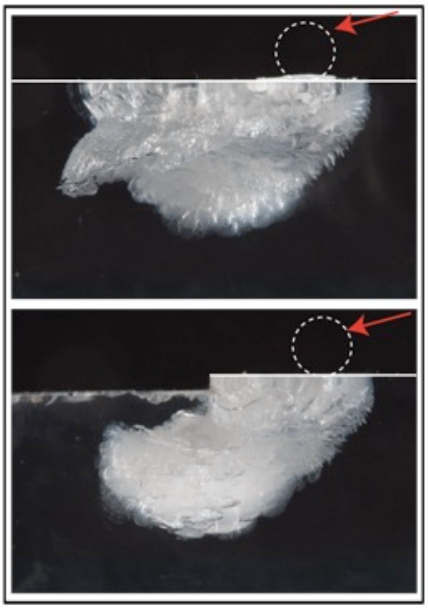

Figure 1. Final damage extent for two equivalent impacts: 0.635-cm aluminum projectile into a planar PMMA target at ~4.8 km/s. Impact angle: 15° from the horizontal; the projectile size is shown for scale, and the white line indicates the top surface of the PMMA block. (top) Impact into an unmodified target; (bottom) impact into PMMA with a surface layer (0.158 cm thick) downrange that was lost during impact.

These new experimental results demonstrate that the failure zone dipping downrange results from strain created by decapitated projectile fragments impacting the target downrange. Projectile decapitation is a fundamental process, especially for highly oblique impacts, that has significant implications for the cratering process [e.g., 6, 10-15], and is easily identifiable for grazing impacts on planetary surfaces (Figure 3). Our experiments reveal another aspect of projectile failure in subsurface damage expression: extended shallow failure downrange (this is also seen in quarter space experiments [16]). Removing the tongue-like feature by decoupling the decapitation/re-impact process results in a damage zone more consistent with numerical simulations (Figure 2), excluding free surface effects. Consequently, numerical models do not yet fully capture all of the processes occurring during oblique impacts.

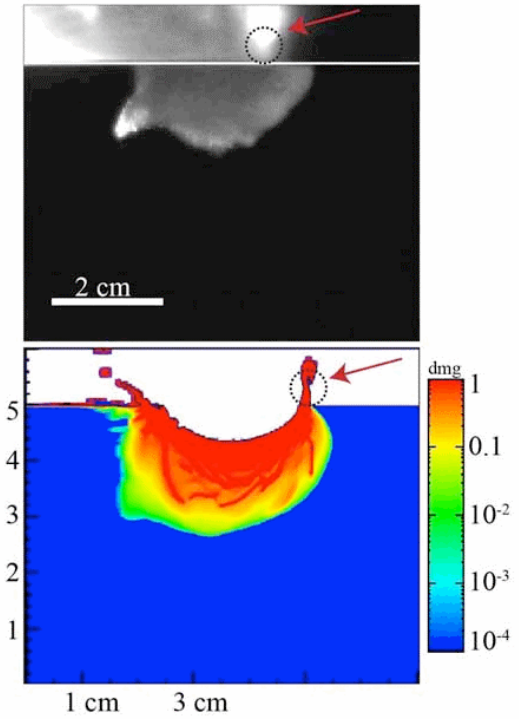

Figure 2. Comparison between laboratory experiment (top) and a CTH model (below) with identical impact conditions. Damage extent is shown at 30 μsec after impact, after the damage had finished growing. Impact of a 0.635-cm aluminum projectile into a planar PMMA target at ~3.9 km/s. Impact angle: 15° from the horizontal; the projectile size is shown for scale. (top) AVGR experiment, the white line indicates the top surface of the PMMA block. (bottom) CTH model showing damage. Failure occurs when dmg=1. Note the absence of diving tongue downrange in the model, even though the overall damage extent below the impact point is similar to the experiment.

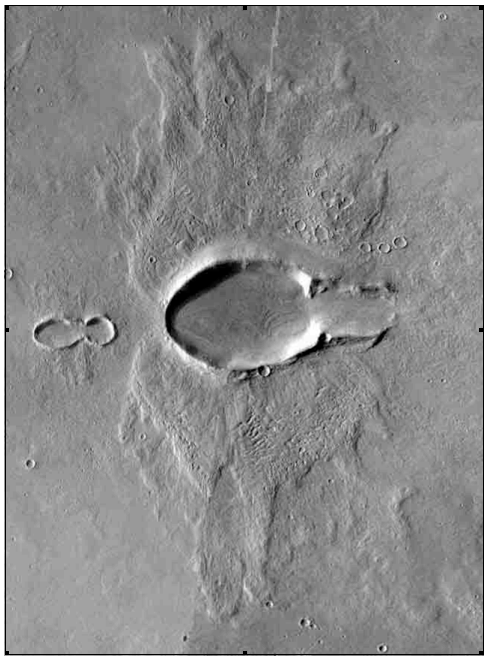

Figure 3. Mosaic of three THEMIS images showing an elongated crater on Mars (V13947003, V30669005 and V12100004). Note the failure pattern downrange resulting from re-impact by pieces of the decapitated projectile (impact is from left to right).

References: [1] Schultz, P. H., and R. R. Anderson (1996), *GSA Special Papers 302,* pp. 397-417; [2] Stickle, A. M., P. H. Schultz, and D. A. Crawford (2009), *LPS XL,* Abstract #2357; [3] Stickle, A. M., and P. H. Schultz (2010), *LPS XLI,* Abstract # 2598; [4] Stickle, A. M., and P. H. Schultz (2011), *Int. J. Imp. Eng.*, *38*(6), 527-534; [5] Schultz, P. H., S. Sugita, C. A. Eberhardy, and C. M. Ernst (2006), *Int. J. Imp. Eng.*, *33*, 771-780; [6] Stickle, A.M. and P.H. Schultz (2011), submitted to *JGR;* [7] McGlaun, J.M. et al. (1990) *Int. J. Imp. Eng.* 10, 351-360; [8] Thompson S. L. & Lauson H. S. (1972) Sandia Technical Report SC-RR-710714; [9] Johnson, G.R. and W.H. Cook (1985) *Eng. Frac. Mech., 21*(1), 31-48; [10] Schultz, P. H., and D. E. Gault (1990), in *Global Catastrophes in Earth History: An Interdisciplinary Conference on Impacts, Volcanism, and Mass Mortality*, edited by V. L. Sharpton and P. D. Ward, pp. 239-261; [11] Schultz, P. H., and D. E. Gault (1990), *LPI Contributions*, *740*, 49; [12] Schultz, P. H., and D. E. Gault (1991), *LPS XXII*, 1195-1196; [13] Orphal, D. L., and C. E. Anderson Jr (2001), *Int. J. Imp. Eng.*, *26*(1-10), pp. 567-578; [14] Schultz, P.H. and A.B. Lutz-Garihan (1982), *J. Geophys. Res, 87,* pp. A84-A86; [15] Herrick, R.R. and N.K. Forsberg-Taylor (2003) *Met. & Planet. Sci., 38*, pp. 1551-1553. [16] Schultz et al. (2007), *Icarus* 190, 295-333.